Available online at www.sciencedirect.com
ScienceDirect
Trans. Nonferrous Met. Soc. China 27(2017) 397−405
Transactions of Nonferrous Metals Society of China
www.tnmsc.cn

Oxidation behavior of C/C composites with SiC/$ZrSiO_4$−SiO_2 coating

Yang LI[1], Peng XIAO[1], Zhuan LI[1] ,Wei LUO[1], Wei ZHOU[1,2]

1. State Key Laboratory for Powder Metallurgy, Central South University, Changsha 410083, China;
2. College of Metallurgy and Material Engineering, Hunan University of Technology, Zhuzhou 412008, China

Received 2 December 2015; accepted 13 June 2016

Abstract: A SiC/$ZrSiO_4$−SiO_2 (SZS) coating was successfully fabricated on the carbon/carbon (C/C) composites by pack cementation, slurry painting and sintering to improve the anti-oxidation property and thermal shock resistance. The anti-oxidation properties under different oxygen partial pressures (OPP) and thermal shock resistance of the SZS coating were investigated. The results show that the SZS coated sample under low OPP, corresponding to the ambient air, during isothermal oxidation was 0.54% in mass gain after 111 h oxidation at 1500 °C and less than 0.03% in mass loss after 50 h oxidation in high OPP, corresponding to the air flow rate of 36 L/h. Additionally, the residual compressive strengths (RCS) of the SZS coated samples after oxidation for 50 h in high OPP and 80 h in low OPP remain about 70% and 72.5% of those of original C/C samples, respectively. Moreover, the mass loss of SZS coated samples subjected to the thermal cycle from 1500 °C in high OPP to boiling water for 30 times was merely 1.61%.
Key words: C/C composite; SiC/$ZrSiO_4$−SiO_2 coating; oxygen partial pressure; anti-oxidation; thermal shock; residual compressive strength

1 Introduction

Carbon/carbon (C/C) composites possess many advantages such as light weight, high strength and modulus at the elevated temperature [1,2]. They are considered to be the potential candidates for high-temperature structures. However, the C/C composites are prone to oxidation in a oxidizing environment above 400 °C [3]. Thus, many investigations on curing Achilles' heel of C/C composites have been carried out for several decades [4−7].

Currently, the coating technology has been regarded as an effective way to protect the C/C composites against oxidation [8]. It is generally known that the silicon carbide (SiC) coating possesses good physical and chemical compatibility to C/C matrix, and is widely used as bonding layer between C/C and outer ceramic layer to provide extra protection for C/C composites [9,10]. However, a single SiC layer cannot provide a long-term protection for C/C matrix [6]. Hence, great efforts were concentrating on the silicon-based multilayer coatings in order to improve the anti-oxidation of C/C composites [11,12]. The zirconium silicate ($ZrSiO_4$) has been considered as a candidate material to apply at high-temperature due to its excellent chemical stability and low coefficient of thermal expansion (4.1×10^{-6}/°C at 1400 °C) [13,14]. SUN et al [15,16] and LIU et al [17] developed a $ZrSiO_4$/SiC coating by hydrothermal electrophoretic deposition which showed a good anti-oxidation as well as the SiC−Si−$ZrSiO_4$ coating systems. It also proved that the $ZrSiO_4$−SiC coating systems offered good solutions for the oxidation protection of C/C composites. However, according to the work of LIU et al [17], SUN et al [15,16] and LI et al [1], the preparation methods for coating systems were pretty complicated. Additionally, most of their investigations were limited in the isothermal oxidation in ambient air. It is well known that the C/C composites suffered to different environments with different oxygen partial pressures (OPP) presented diversity in properties at high temperature during the potential applications [18,19]. Hence, the silicon-based coating systems subjected to different OPP at high temperature should be comprehensively studied. In the present work, the SZS coating was simply prepared by combination of pack cementation for SiC inner coating and slurry painting then sintered for $ZrSiO_4$−SiO_2 out coating. The anti-

Foundation item: Project supported by the Nonferrous Metal Oriented Advanced Structural Materials and Manufacturing Cooperative Innovation Center, China; Project (51205417) supported by the National Natural Science Foundation of China
Corresponding author: Peng XIAO; Tel: +86-731-88830131; E-mail: xiaopengcsu@csu.edu.cn
DOI: 10.1016/S1003-6326(17)60045-1

oxidation of SZS coating at 1500 °C in high OPP (air flow rate: 36 L/h) and low OPP (ambient air), was systematically investigated. Additionally, the microstructures, residual compressive strength after oxidation test and thermal shock resistance from 1500 °C in high OPP (air flow rate: 36 L/h) to boiling water were studied to evaluate the performance of the SZS coating system. The current study aims to provide some valuable information for the further research in the protection of C/C composites at the elevated temperature under different oxygen partial pressures.

2 Experimental

2.1 Preparation of coatings

The small specimens (10 mm × 10 mm × 10 mm) with the density of 1.67 to 1.70 g/cm^3 as substrates were cut from the bulk 2.5-dimensional C/C composites, which were prepared by chemical vapor infiltration. The C/C specimens were polished by using 200, 600 and 1000 grit SiC paper, successively, then followed by water cleaning and drying at 120 °C for 2 h. The powder composition for pack cementation included: 60%−65% Si, 5%−10% carbon black, 10%−30% β-SiC and 0−5% Al_2O_3 (mass fraction). All the powders (analytical grade) were mixed by ball-milling for 2 h in ethanol solution. The C/C composite specimens and the powder mixtures were placed in a graphite crucible, and heated to 1750 °C in an argon atmosphere and then held at 1750 °C for 2 h to form the SiC coating. After the preparation of SiC layer, the $ZrSiO_4$−SiO_2 coating was obtained on the as-prepared SiC coating surface by slurry painting and sintering method. The slurry painting composition in this procedure included: 20%−60% SiO_2, 30%−60% ZrO_2 and 0−5% sinter aids (mass fraction). All the powders were analytically graded and mixed by ball-milling with a ethanol solution containing 3% polyvinyl alcohol for 2 h. After slurry painting process, the coated specimens were dried at 100 °C and then sintered at 1500 °C under argon atmosphere for 1 h to form the $ZrSiO_4$−SiO_2 coating.

2.2 Isothermal oxidation test

The samples with SiC and SZS coatings were tested at 1500 °C in low OPP (ambient air) or high OPP (air flow air: 36 L/h) in a corundum tube furnace (tube diameter: 10 cm, Length: ~100 cm) to investigate the isothermal oxidation behavior. The cumulative mass change rates (Δw) of the specimens were described by the following expression and were reported as a function of time:

$$\Delta w = \frac{m_i - m_0}{m_0} \times 100\% \quad (1)$$

where m_0 and m_i are measured by an electronic balance with a sensitivity of ±0.1 mg and represent the masses of the specimens before and after oxidation, respectively.

2.3 Thermal shock test

The thermal shock test was performed on the SZS coated C/C composites samples from 1500 °C in high OPP to boiling water. The specimens were placed into the corundum tube furnace and heated at 1500 °C for 3 min. Subsequently, the specimens were poured into the boiling water (about 100 °C) to cool down quickly to room temperature. Finally, after 2 h drying at 100 °C in the oven, the masses of specimens were measured by electronic balance with sensitivity of ±0.1 mg, and the mass loss was calculated by Eq. (1). The above steps were repeated 30 times.

2.4 Characterization

According to ASTM C1258−97, the compressive tests for the residual strength of specimens after oxidation were carried out on a universal testing machine (Instron 1196) with a loading rate of 1 mm/min. The microstructures and the phase composition of the SiC and SZS coatings were characterized by scanning electron microscopy (SEM, FEI Nova Nano SEM−230) with energy dispersive X-ray spectroscopy and X-ray diffraction (XRD) analyzer (Rigaku Ltd., Japan), respectively.

3 Results and discussion

3.1 Phase compositions and microstructures of coatings

Figure 1 shows the XRD patterns of the as-prepared SiC coating and SZS coating. As shown in Fig. 1, the SiC coating is composed of α-SiC and β-SiC, and the SZS coating is composed of $ZrSiO_4$ and residual SiO_2 after the

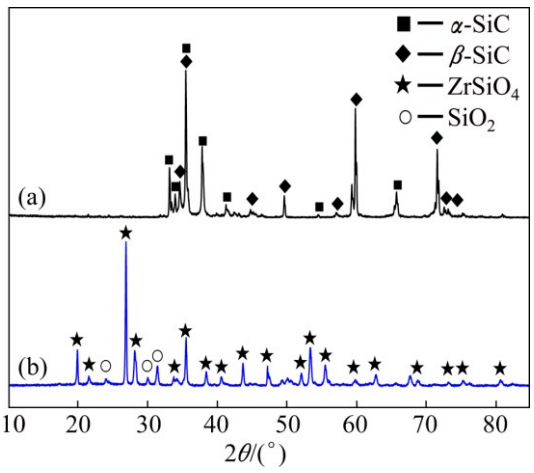

Fig. 1 XRD patterns of SiC and SZS coatings: (a) SiC coating; (b) SZS coating after sintering

slurry painting and sintering processes. Generally, the SiO_2 in the coating systems could improve the oxidation property by self-healing.

Figures 2(a) and (b) exhibit the surfaces and cross-section microstructures of the SiC coated sample. As shown in Fig. 2(a), the SiC coating is composed of fine and dense aggregates which are almost uniform and smaller than 1 μm in diameter. Additionally, the SiC coating surface is fairly rough, which is beneficial to improving the adhesion between outer coatings and SiC inner coating. As shown in Fig. 2(b), many pores were observed in the cross-section of SiC coating. Generally, these pores could effectively ease the thermal stress caused by mismatch of the coefficient of thermal expansion at the elevated temperature. Figure 2(c) exhibits the morphology of the SZS coated sample. It is observed that the SZS coating surface is pretty dense with some micro-cracks. Moreover, it is seen that the SZS coating comprises a glass-like phase and bump grains. The EDS analysis results of spot *A* and spot *B* marked in Fig. 2(c) are presented in the Figs. 2(e) and (f), respectively. The results indicate that the glass-like phase in Fig. 2(c) is mainly composed of SiO_2, while the bump grains are mainly composed of $ZrSiO_4$. Furthermore, the

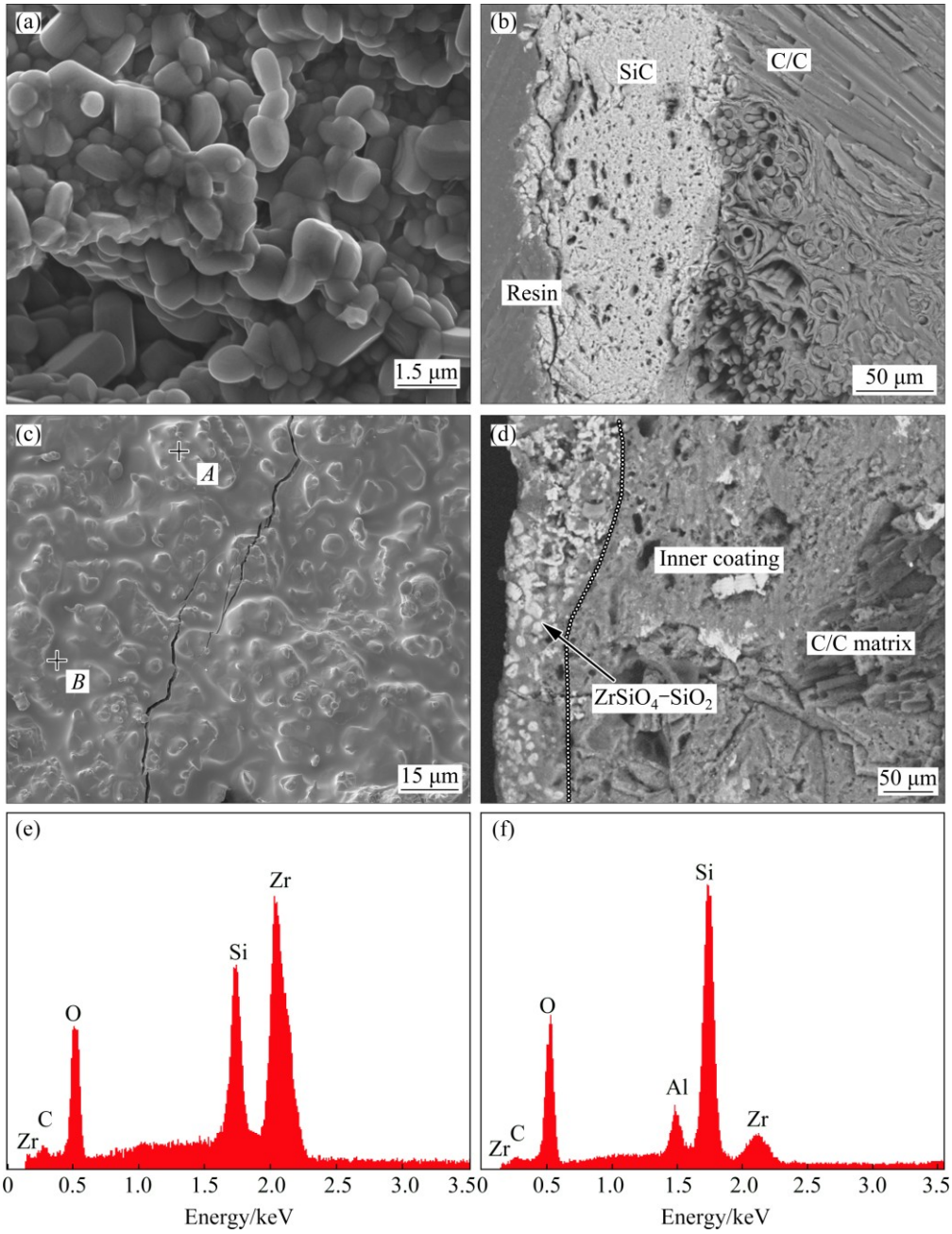

Fig. 2 SEM images and element line scanning results of as-prepared coatings: (a) Surface micrograph of SiC coating; (b) Cross-section micrograph of SiC coating; (c) Surface micrograph of SZA coating; (d) Cross-section micrograph of SZS coating; (e, f) EDS analysis result of spots *A* and *B* in Fig. 2(c), respectively

cross-section micrograph of SZS coating is displayed in Fig. 2(d). The obvious two layers are obviously observed in the SZS coating. Figure 2(d) also indicates that the adhesion and compatibility between inner and outer coatings are pretty good. Note that the dense $ZrSiO_4$−SiO_2 coating presents a mosaic-like structure that $ZrSiO_4$ is embedded into SiO_2 glass. The phase distribution in such mosaic structure is conducive to relieve thermal stress caused by the diversity of CTE (coefficient of thermal expansion) between $ZrSiO_4$ and SiO_2. Therefore, the SZS coating is expected to have a good resistance to oxidation and thermal shock.

3.2 Oxidation resistance of coating systems

The isothermal oxidation curves of the SiC and SZS coated samples in low OPP at 1500 °C are shown in Fig. 3. As shown in Fig. 3(a), the SiC coating cannot provide a long-time protection for the C/C matrix. The mass loss rate of the SiC-coated C/C samples is about 2.1% after oxidation at 1500 °C under low OPP for 58 h. However, the SZS-coated C/C exhibits a mass gain rate of 0.54% after 111 h in low OPP at 1500 °C. In comparison, the SZS coating system obviously shows a better anti-oxidation property under low OPP at 1500 °C than single SiC coating.

As for the silicon-based coating at high temperature, the oxidation kinetic is generally determined by the diffusion rate of the oxygen along the molten layers [19]. The diffusion behavior of O_2 can be expressed by Fick's first and second laws as Eqs. (2) and (3) [20,21].

$$J = -D\frac{\mathrm{d}C}{\mathrm{d}t} \tag{2}$$

$$\frac{\partial C(x,t)}{\partial t} = D\frac{\partial^2 C(x,t)}{\partial x^2} \tag{3}$$

where J is the flux density of O_2, D is the diffusion coefficient, and C is the concentration of O_2.

Based on the oxidation curves as shown in Fig. 3, the oxidation behavior of SiC coating and SZS coating can be divided into two main stages (parabolic oxidation stage and non-parabolic oxidation stage) as shown in Figs. 3(b) and (c), respectively. The corresponding oxidation kinetic equation in the parabolic stage can be described, as shown in Eqs. (4) and (5). Among which x is the oxidation time, y is the mass loss rate, R is the association coefficient and a, b are constants, respectively.

As for the SiC coated C/C composites under low OPP:

$$y=0.023x^2-0.146x+8.18\times10^{-4}\ (0<x\leq4\ \text{h},\ R=0.999) \tag{4}$$

As for the SZS coated C/C at 1500 °C under low OPP:

$$y=0.0098x^2-0.114x+1.358\times10^{-5}\ (0<x\leq6\ \text{h},\ R=0.999) \tag{5}$$

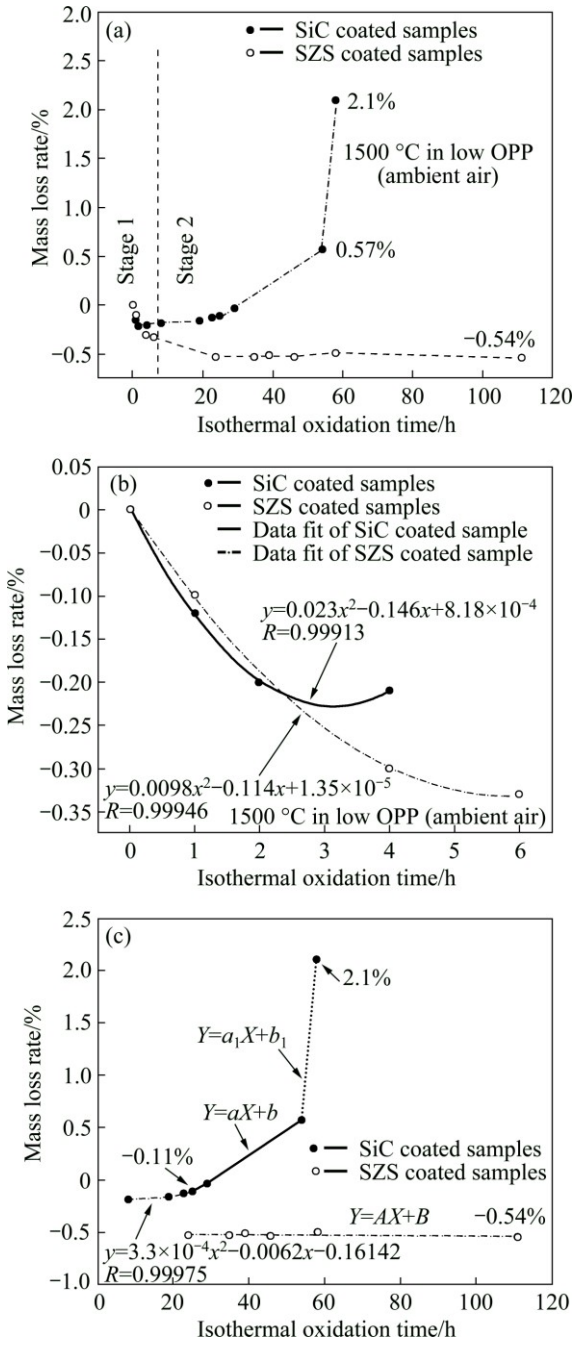

Fig. 3 Isothermal oxidation curves of SiC and SZS coated C/C composites in low OPP (ambient air) at 1500 °C: (a) Isothermal oxidation curve of coated sample; (b) Stage 1 in Fig. 3(a); (c) Stage 2 in Fig. 3(a)

Both the mass changes of coatings versus the oxidation time under low OPP at 1500 °C, as shown in Fig. 3(b), follow the parabolic rate law. Figure 3(b) indicates that the as-prepared coatings exhibit pretty good anti-oxidation performance in the initial oxidation experience (SiC coating: 0−25 h, and SZS coating: 0−6 h). Meanwhile, the oxidation of the SZS and SiC coated C/C samples is mainly controlled by the diffusion of oxygen. The oxidation in this stage can be described in Eqs. (6) and (7)

$$SiC(s)+2O_2=SiO_2(s)+CO_2(g) \quad (6)$$

$$2SiC(s)+3O_2=2SiO_2(s)+2CO(g) \quad (7)$$

After the isothermal oxidation at 1500 °C for 25 h, the mass loss rate of the SiC-coated sample inclines to increase linearly with increased oxidation time. At this point, the generated SiO_2 cannot seal the cracks and pores well. On the one hand, it was caused by the volatilization of the molten SiO_2 at high temperature [22]. On the other hand, the CO and CO_2 gas as mentioned in Eqs. (6) and (7) will result in new defects such as cracks and pores during their escape from the interface between SiC and $ZrSiO_4$−SiO_2 coatings to the surface. Obviously, these new defects could lead to a quick diffusion of oxygen into the matrix. As shown in Fig. 4, after oxidation for 35 h, the SiC phase on the surface of SiC-coated sample can also be detected, which indicates that the SiO_2 layer is not thick and dense enough owing to the above-mentioned two reasons.

As for the SZS-coated samples, the defects in the coating are sealed by the molten SiO_2 in the parabolic stage (0−6 h). In general, the diffusion rates of oxygen in SiO_2 and $ZrSiO_4$ are quite low [23]. Therefore, the mass change of SZS-coated C/C sample reaches constant, which indicates that the mass gain rate from oxidation of SiC is almost equal to the mass loss rate from the volatilization of SiO_2. Moreover, the mosaic-like structure of coating as shown in Figs. 2(b) and (c) can effectively decrease the volatilization rate. As shown in Fig. 4, the main phases in the SZS coating after oxidation for 46 h are still $ZrSiO_4$ and SiO_2. When compared with Fig. 1, the characteristic peaks of SiO_2 become stronger, which indicates a higher content of SiO_2 in the SZS coating.

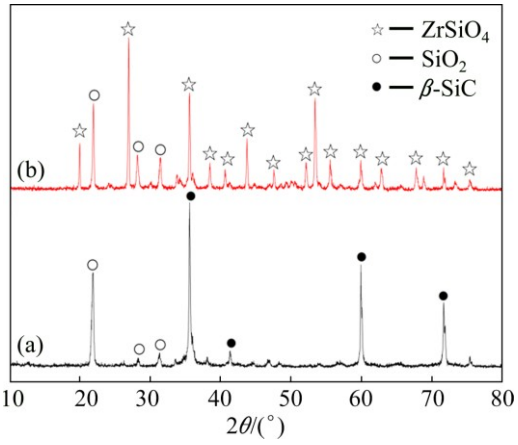

Fig. 4 XRD patterns of coatings after oxidation at 1500 °C under low OPP: (a) SiC coating after oxidation for 35 h; (b) SZS coating after oxidation for 46 h

Figure 5 shows the surface and cross-section morphologies of SZS-coated C/C under low OPP at 1500 °C. As shown in Fig. 5(a), the dense glass layer on the surface after oxidation after 46 h at 1500 °C is pretty smooth. Note that the glass layer covers the sample without apparent holes and big cracks. As shown in Fig. 5(b), some defects in the SiC coating and the SiC/$ZrSiO_4$−SiO_2 interface can be observed on the cross-section of the SZS coating systems due to the shift and expansion of the gas generated from the oxidation of SiC at high temperature. However, the interfaces between SiC and C/C, SiC and $ZrSiO_4$−SiO_2 are still in fairly good adhesions, which prove that the SZS coating can protect the C/C matrix at 1500 °C under the low OPP for a longer time.

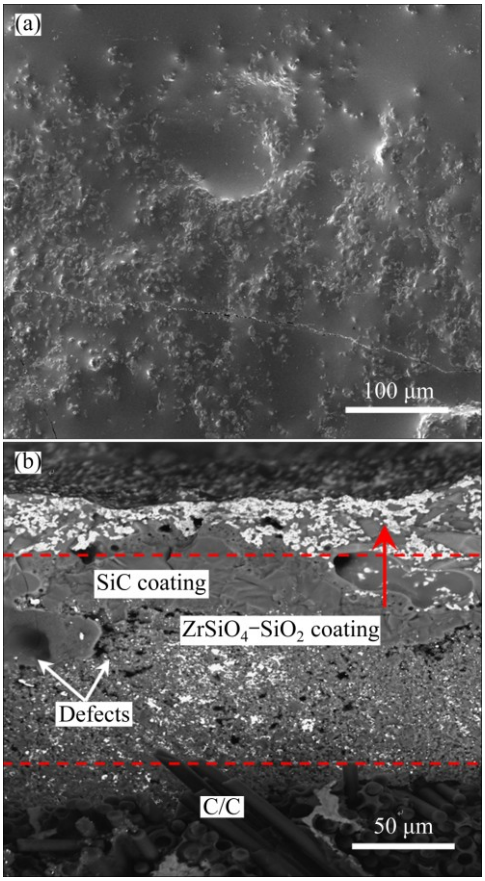

Fig. 5 Surface and cross-section morphologies of SZS-coated C/C under low OPP at 1500 °C for 46 h: (a) SEM image of surface; (b) SEM image of cross-section

Figure 6 shows the isothermal oxidation curve of the SZS-coated C/C composites under high OPP (flow air: 36 L/h) at 1500 °C. As illustrated in Fig. 6(a), the SZS coating exhibits a good anti-oxidation property. After oxidation at 1500 °C for 50 h under high OPP, the SZS-coated sample did not suffer an obvious mass loss (merely about 0.03%).

Figure 6(b) shows the parabolic oxidation stage at 1500 °C marked in Fig. 6(a). The corresponding oxidation kinetic equation can be described as Eq. (8). Among which x is the oxidation time, y is the mass loss

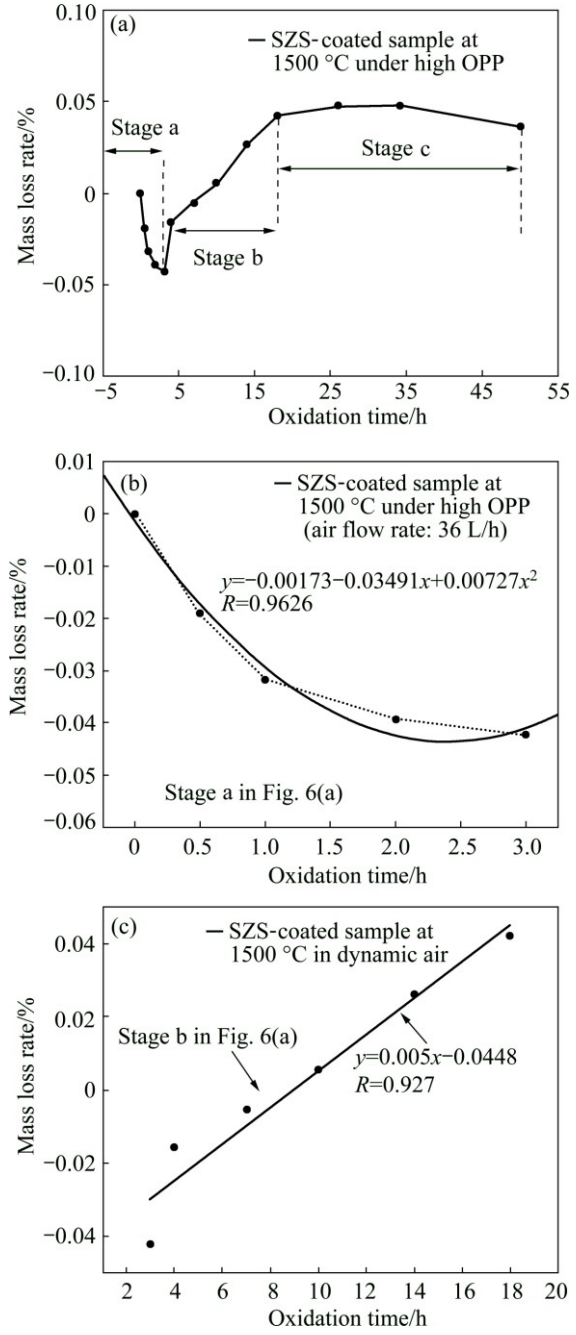

Fig. 6 Isothermal oxidation curves of SZS-coated C/C composites under high OPP at 1500 °C: (a) Isothermal oxidation curve; (b) Parabolic oxidation stage in Fig. 6(a); (c) Stage b in Fig. 6(a)

rate, R is the association coefficient and a, b are constants respectively.

As for the SZS-coated C/C at 1500 °C under high OPP:

$$y=0.00727x^2-0.0349x+1.7\times10^{-3}\ (0<x\leq3\ \text{h},\ R=0.962) \quad (8)$$

Generally, the mass gain of SiC/$ZrSiO_4$−SiO_2-coated C/C composites is mainly caused by the oxidation of SiC. As previously shown in Fig. 3(b), the oxidation of SiC coating obeys the parabolic rate law well. The oxidation rate of SiC is determined by diffusion rate of oxygen. Similarly, when the SZS coating is totally exposed in air at the initial time of oxidation, it could result in a mass gain from the oxidation of SiC into SiO_2 with a fast rate. As the oxidation proceeds, the SiC is covered by the SiO_2 with the increased thickness. Furthermore, the defects on the surface are gradually sealed by the molten SiO_2, which makes the oxygen more difficult to diffuse towards to the matrix. As a result, the slope of the mass gain as shown in Fig. 6(b) decreases gradually.

Figure 6(c) shows the stage b as marked in Fig. 6(a). It is seen that the mass change of the SZS-coated sample as shown in Fig. 6(c) could follow the linear Eq. (9):

$$y=0.005x-0.0448\ (3<x\leq18\ \text{h},\ R=0.927) \quad (9)$$

where x is the oxidation time, y is the mass loss, R is the association coefficient, respectively.

In stage b, the molten SiO_2 at high temperature can effectively seal the defects in the SZS coating. Moreover, the mass loss from oxidation of carbon and the mass gain from oxidation of SiC are in equilibrium. The volatilization of SiO_2 in this stage is mainly responsible for the mass changes. As the oxidation proceeds, the oxygen will gradually diffuse into the coating to react with SiC or C when the SiO_2 layer in the outer surface is not thick enough. The oxidation process will lead to the new generation of CO and CO_2 gas [24,25]. Afterwards, the pores with big sizes at the interface as shown in Fig. 7(b) will be generated owing to expansion of the CO and CO_2 gases. These pores were inevitably generated on the surface of the SZS coated C/C composites after the escape of CO and CO_2 gases. Note that the dynamic air can accelerate the volatilization of SiO_2 at 1500 °C [26]. Therefore, the SiO_2 in the SZS coating in stage c is not so sufficient as before. Consequently, the above-mentioned defects could not be sealed quickly. Hence, these defects including the pores after cooling down can be observed as shown in Fig. 7(a).

Additionally, as shown in Fig. 6(a), the mass gain and the mass loss in stage c are in equilibrium. Therefore, the SZS coated sample presents a tiny mass loss rate (about 0.03%) after oxidation at 1500 °C for 50 h under high OPP. It is clear that the SZS coating shows a good oxidation resistance at 1500 °C under high OPP.

It is noteworthy that the microstructures of the SZS-coated samples vary with OPP at 1500 °C. Compared with microstructures of the SZS-coated sample tested in high OPP at 1500 °C, the SZS-coated sample which experienced 46 h in low OPP presented a better combination between the inner−outer coatings and coating/matrix. Moreover, less pores were observed in the area of interface between the internal/external coatings when the SZS-coated sample is subjected to the low OPP at 1500 °C. Generally, the molten SiO_2 could

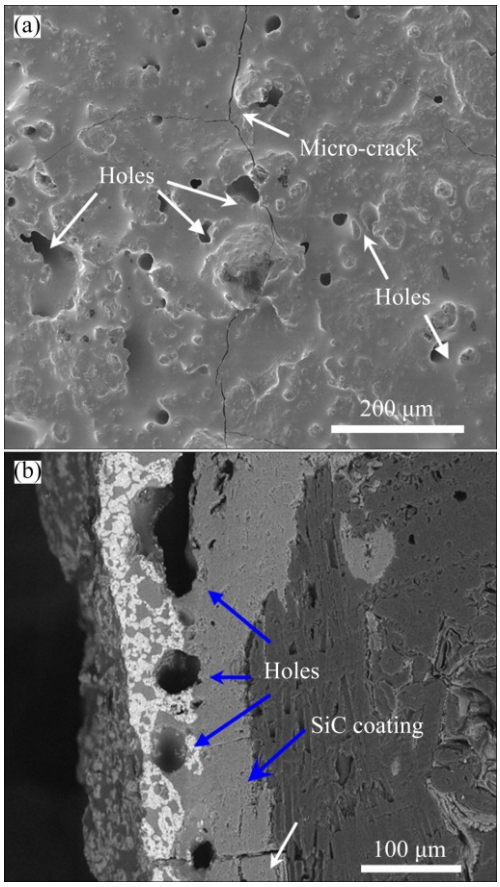

Fig. 7 Surface and cross-section morphologies of SZS-coated C/C in dynamic air (0.6 L/min) at 1500 °C for 50 h: (a) Surface SEM image; (b) Cross-section SEM image

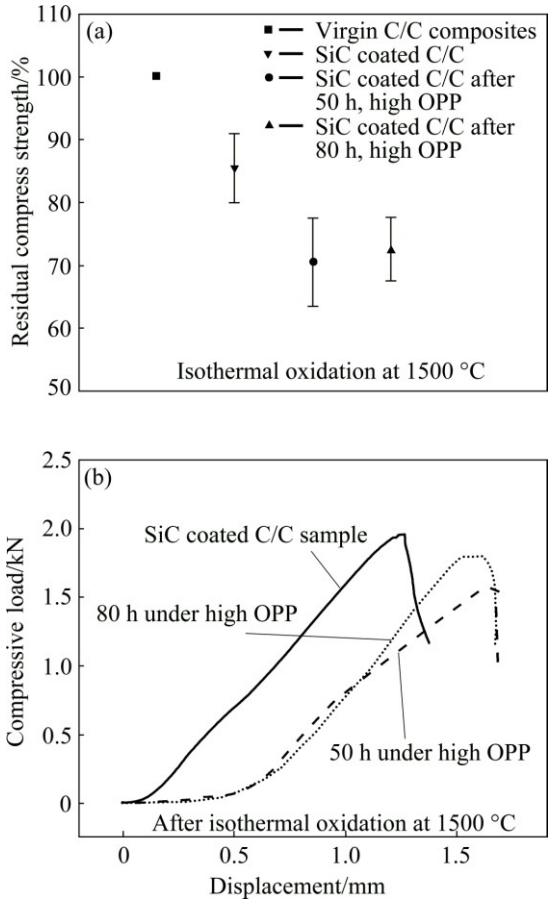

Fig. 8 Residual strength and typical load−displacement curves after oxidation at 1500 °C: (a) Diagram of residual compressive strength; (b) Load−displacement curves of oxidized samples

fill the defects like pores and cracks in the SZS coating. Additionally, these cracks usually close at elevated temperatures. Hence, the content of molten SiO_2 in the SZS coating after oxidation should be responsible for these differences in microstructures. The air flow could probably accelerate the volatilization of molten SiO_2 at 1500 °C and the defects like cracks and pores in the coating cannot be effectively self-sealed under high OPP. More defects in the coating resulted in a higher diffusion rate of oxygen into the C/C matrix, which corresponds to a faster oxidation of carbon. More oxidation of carbon will result in more CO_2 and CO gases which are detrimental to the coating systems.

Figure 8 shows the residual compressive strength (RCS) and the load−displacement curves of the SiC- or SZS-coated samples. As shown in Fig. 8(a), the RCS of SZS-coated samples without oxidation decreases to about 85% of that of the virgin C/C owing to the thermal- damage on carbon fiber at high processing temperature and the corrosion of liquid Si infiltration into the C/C matrix. Additionally, the RCSs of SZS-coated C/C after oxidation for 50 h under high OPP and 80 h under low OPP are approximately 70% and 72.5% of that of the virgin C/C matrix, respectively. The oxidation and thermal damage of C/C matrix could be responsible for the mechanical degradation of the SZS-coated samples.

Figure 8(b) shows the typical load−displacement curves of the virgin C/C composites and SZS-coated sample after oxidations. It is seen that the virgin C/C sample shows a nearly linear behavior to the compressive stress, and then breaks rapidly when the maximum stress achieves. As for the SZS-coated sample, the similar fracture as C/C sample can be observed. However, the SZS-coated sample after oxidation show about 0.5 mm longer displacement because of the additional thickness of the SZS coating (the thickness of SZS coating after oxidation is about 0.25 mm as shown in Fig. 5). Additionally, the weak load (about 45 N) in initial stage (from 0 to approximately 0.5 mm of the displacement) is mainly responsible for the deformation of the SZS coating, because the SZS coating after oxidation is brittle, and cannot carry load as high as the C/C matrix.

In conclusion, the SZS coating shows a pretty good anti-oxidation performance at 1500 °C under low

OPP and high OPP.

3.3 Thermal shock resistance of SiC/$ZrSiO_4$−SiO_2 coating

The thermal shock resistance of SZS coating was evaluated by thermal cycling oxidation between 1500 °C and boiling water. The mass loss curve of the SZS-coated samples after the thermal shock tests is presented in Fig. 9. It is seen that the SZS coating exhibits a good resistance to the thermal shock from 1500 °C to boiling water. After 30 times of thermal cycling, the mass loss rate of the SZS-coated samples is merely 1.61%. Additionally, the curve of mass loss during the thermal cycling can be characterized as a straight line fitted according to the equation (y=Ax+B) and association coefficient (R) as shown in Fig. 9.

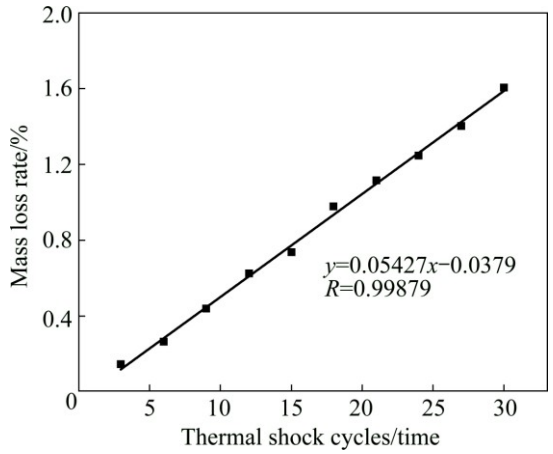

Fig. 9 Thermal cycling oxidation curve of SZS-coating coated C/C composites between 1500 °C and boiling water

4 Conclusions

1) The SZS coating shows a good anti-oxidation behavior in a long term. It can effectively protect the C/C matrix from oxidation at 1500 °C for 111 h under low OPP, corresponding to the ambient air, with a mass gain rate of 0.54%, and mass loss rate of 0.03% after 50 h oxidation at 1500 °C in high OPP, corresponding to the air flow rate of 36 L/h, respectively.

2) The residual strengths of the coated sample after oxidation for 50 h under high OPP and for 80 h under low OPP are about 70% and 72.5% of that of the virgin C/C, respectively.

3) The SZS coating presents a good thermal shock resistance. The mass loss of SZS coated samples subjected to the thermal cycle from 1500 °C under high OPP to boiling water for 30 times is merely 1.61%.

Acknowledgements

We would like to express our heartfelt gratitude to Mr. Fan JIA, Mr. Heng LUO and Mr. F. REICHERT for their linguistic assistances during the preparation of this manuscript.

References

[1] LI Ke-zhi, SHEN Xue-tao, LI He-jun, ZHANG Shou-yang, FENG Tao. Ablation of the carbon/carbon composite nozzle-throats in a small solid rocket motor [J]. Carbon, 2011, 49(4): 1208−1215.

[2] PENG Li-na, HE Guo-qiang, LI Jiang, WANG Lei, QIN Fei. Effect of combustion gas mass flow rate on carbon/carbon composite nozzle ablation in a solid rocket motor [J]. Carbon, 2012, 50(4): 1554−1562.

[3] GUO Wei-ming, XIAO Han-ning, YASUDA E, CHENG Yin. Oxidation kinetics and mechanisms of a 2D-C/C composite [J]. Carbon, 2006, 44(15): 3269−3276.

[4] JACOBSON N S, LEONHARDT T A, CURRY D M, RAPPD R A. Oxidative attack of carbon/carbon substrates through coating pinholes [J]. Carbon, 1999, 37(3): 411−419.

[5] SMEACETT F, SALVO M, FERRARIS M. Oxidation protective multilayer coatings for carbon–carbon composites [J]. Carbon, 2002, 40(4): 583−587.

[6] JACOBSON N S, ROTH D J, RAUSER R W, CAWLEY J D, CURRY D M. Oxidation through coating cracks of SiC-protected carbon/carbon [J]. Surface and Coatings Technology, 2008, 203(3): 372−383.

[7] FU Qian-gang, LI He-jun, WANG Yong-jie, LI Ke-zhi, WU Heng. A Si–SiC oxidation protective coating for carbon/carbon composites prepared by a two-step pack cementation [J]. Ceramics International, 2009, 35(6): 2525−2529.

[8] YAN Zhi-qiao, XIONG Xiang, XIAO Peng, CHENG Feng, ZHANG Hong-bo, HUANG Bo-yun. Oxidation behavior of oxidation protective coatings for C/C−SiC composites at 1500 °C [J]. Transactions of Nonferrous Metals Society of China, 2009, 19(1): 61−64.

[9] ZHANG Yu-lei, LI He-jun, FU Qian-gang, LI Ke-zhi, WEI Jian, WANG Peng-yun. A C/SiC gradient oxidation protective coating for carbon/carbon composites [J]. Surface and Coatings Technology, 2006, 201(6): 3491−3495.

[10] WANG Kai-tong, CAO Li-yun, HUANG Jian-feng, FEI Jie. A mullite/SiC oxidation protective coating for carbon/carbon composites [J]. Journal of the European Ceramic Society, 2013, 33(33): 191−198.

[11] ZHANG Yu-lei, LI He-jun, HU Zhi-xiong, LI Ke-zhi, ZHANG Lei-lei. C/SiC/$MoSi_2$−SiC−Si multilayer coating for oxidation protection of carbon/carbon composites [J]. Transactions of Nonferrous Metals Society of China, 2013, 23(7): 2118−2122.

[12] FU Qian-gang, ZHANG Jia-ping, ZHANG Zheng-zhong, LI He-jun, SUN Can. SiC−$MoSi_2$/ZrO_2−$MoSi_2$ coating to protect C/C composites against oxidation [J]. Transactions of Nonferrous Metals Society of China, 2013, 23(7): 2113−2117.

[13] SUN Can, LI He-jun, FU Qian-gang, ZHANG Jia-ping. Microstructure and ablation properties of carbon/carbon composites modified by $ZrSiO_4$ [J]. Corrosion Science, 2014, 79: 100−107.

[14] KAISER A, LOBERT M, TELLE R. Thermal stability of zircon ($ZrSiO_4$) [J]. Journal of the European Ceramic Society, 2008, 28(11): 2199−2211.

[15] SUN Can, LI He-jun, FU Qian-gang, LI Hai-liang, WANG Yong-jie, WU Heng. $ZrSiO_4$ oxidation protective coating for SiC-coated carbon/carbon composites prepared by supersonic plasma spraying [J]. Journal of Thermal Spray Technology, 2013, 22(4): 525−530.

[16] SUN Can, LI He-jun, LUO Hui-juan, XIE Jing, ZHANG Jia-ping, FU Qian-gang. Effect of Y_2O_3 on the oxidation resistant of $ZrSiO_4$/SiC coating prepared by supersonic plasma spraying technique for carbon/carbon composites [J]. Surface and Coatings

Technology, 2013, 235(0): 127−133.

[17] LIU Jia, CAO Li-Yun, HUANG Jian-feng, XIN Yu, YANG Wen-dong, FEI Jie, YAO Chun-yan. A $ZrSiO_4$/SiC oxidation protective coating for carbon/carbon composites [J]. Surface and Coatings Technology, 2012, 206(14): 3270−3274.

[18] ZOU Bing-lin, HUI Yu, HUANG Wen-zhi, ZHAO Su-mei, CHEN Xiao-long, XU Jia-ying, TAO Shun-yan, WANG Ying, CAI Xiao-Long, CAO Xue-qiang. Oxidation protection of carbon/carbon composites with a plasma-sprayed ZrB_2−SiC−Si/Yb_2SiO_5/$LaMgAl_{11}O_{19}$ coating during thermal cycling [J]. Journal of the European Ceramic Society, 2015, 35(7): 2017−2025.

[19] ZHANG Yong-liang, HUANG Jian-feng, LI Cui-yan, CAO Li-yun, OUYANG Hai-bo, ZHANG Bo-ye, HAO Wei, WANG Wen-jing, YAO Chun-yan. A glass coating prepared by pulse arc discharge deposition for oxidation protection of carbon/carbon composites [J]. Applied Surface Science, 2014, 316: 207−213.

[20] FRITZE H, JOJIC J, WITKE T, RÜSCHER C, WEBER S, SCHERRER S, WEISS R, SCHULTRICH B, BORCHARDT G. Mullite based oxidation protection for SiC−C/C composites in air at temperatures up to 1900 K [J]. Journal of the European Ceramic Society, 1998, 18(16): 2351−2364.

[21] FERES R, YABLONSKY G. Probing surface structure via time-of-escape analysis of gas in Knudsen regime [J]. Chemical Engineering Science, 2006, 61(24): 7864−7883.

[22] YAN Zhi-qiao, XIONG Xiang, XIAO Peng, CHENG Feng, ZHANG Hong-bo, HUANG Bo-yun. A multilayer coating of dense SiC alternated with porous Si–Mo for the oxidation protection of carbon/carbon silicon carbide composites [J]. Carbon, 2008, 46(1): 149−153.

[23] HEITJANS P, KÄRGER J. Diffusion in condensed matter: Methods, materials, models [J]. Diffusion in Condensed Matter Methods, 2005, 50(10):1848−1851.

[24] ZHANG Yu-lei, LI He-jun, YAO Xi-yuan, LI Ke-zhi, ZHANG Shou-yang. C/SiC/Si−Mo−B/glass multilayer oxidation protective coating for carbon/carbon composites [J]. Surface and Coatings Technology, 2011, 206(2−3): 492−496.

[25] LI Ting, LI He-jun, SHI Xiao-hong, CHENG Jing, LIU Lei. Mo−Si−Al−C multiphase oxidation protective coating for carbon/carbon composites [J]. Applied Surface Science, 2013, 276: 154−158.

[26] LAMOREAUS R H, HILDENBRAND D L, BREWER L. High-temperature vaporization behavior of oxides II. Oxides of Be, Mg, Ca, Sr, Ba, B, Al, Ga, In, Tl, Si, Ge, Sn, Pb, Zn, Cd, and Hg [J]. Journal of Physical and Chemical Reference Data, 1987, 16(3): 419−443.

炭/炭复合材料表面 $SiC/ZrSiO_4$−SiO_2 复合涂层的氧化行为

李 杨[1]，肖 鹏[1]，李 专[1]，罗 威[1]，周 伟[1,2]

1. 中南大学 粉末冶金国家重点实验室，长沙 410083；
2. 湖南工业大学 冶金与材料工程学院，株洲 412008

摘 要：为提高炭/炭(C/C)复合材料的高温抗氧化性，采用包埋–刷涂法在其表面制备 $SiC/ZrSiO_4$−SiO_2 (SZS)复合涂层。研究 SZS 复合涂层包覆 C/C 复合材料在 1500 °C 下不同氧分压测试环境下的抗氧化性能以及 1500 °C 至沸水(100 °C)的热循环性能。结果表明：SZS 复合涂层试样具有优异的高温抗氧化性能和热震性能。在 1500 °C 等温高氧分压环境下(空气流量 36 L/h)氧化 50 h 后试样仅轻微失重(约 0.03%)， 而在 1500 °C 低氧分压(静态空气)中氧化 111 h 后仍然增重 0.54%。此外，SZS 复合涂层试样在高氧分压下氧化 50 h 及低氧分压下氧化 80 h 后，其残余压缩强度分别为 70%和 72.5%。SZS 复合涂层试样在经历 30 次热循环以后，其质量损失率仅为 1.61%，残余压缩强度约为 74%。SZS 涂层表现出良好的抗氧化性能和抗热震性能，可在高温下为 C/C 复合材料提供长期的保护。

关键词：C/C 复合材料；$SiC/ZrSiO_4$−SiO_2 复合涂层；氧分压；抗氧化性能；热震性能；残余压缩强度

(Edited by Yun-bin HE)